Research Article

BIOMEDICAL Journal of Scientific & Technical Research

ISSN: 2574 -1241

DOI: 10.26717/BJSTR.2023.51.008066

# Improved Particle Swarm Optimization for Solving in PID Control of Electro-Hydraulic Servo System

**Wen-sheng Xiao[1,2], Guang-xin Li[1,2], Chao Liu[1,2]* and Li-ping Tan[1,2]**

[1]*National Engineering Lab of Offshore Geophysical & Exploration Equipment, China University of Petroleum, China*

[2]*School of Electrical and Mechanical Engineering, China University of Petroleum, China*

***Corresponding author:** Chao Liu, National Engineering Lab of Offshore Geophysical & Exploration Equipment, China University of Petroleum, School of Electrical and Mechanical Engineering, China University of Petroleum, Qingdao 266580, China

**ARTICLE INFO**

**Received:** June 13, 2023

**Published:** June 23, 2023

**Citation:** Wen-sheng Xiao, Guang-xin Li, Chao Liu and Li-ping Tan. Improved Particle Swarm Optimization for Solving in PID Control of Electro-Hydraulic Servo System. Biomed J Sci & Tech Res 51(2)-2023. BJSTR. MS.ID.008066.

**ABSTRACT**

The drill pipe handling system is characterized by large working load, wide range of load variation and high control accuracy requirements, which put certain requirements on the stability and reliability of the hydraulic system. In this paper, the research on the optimized control of electro-hydraulic servo system of drill pipe handling system is mainly conducted. Firstly, the mathematical model of the electro-hydraulic servo system is established, and the transfer function of the electro-hydraulic servo system is solved. Secondly, the Cauchy mutation mechanism is introduced to improve the traditional particle swarm optimization (PSO) algorithm for the defects of local optimum, and the algorithm is verified by a series of experiments. The results show that the improved PSO has faster convergence speed and higher convergence accuracy, and the solution performance is greatly improved. Finally, Simulink is used to build a simulation model and the improved PSO algorithm is applied to the optimization of PID parameters. It is found that the improved PSO algorithm obtains better control effect through simulation.

**Keywords:** Drill Pipe Handling System; Electro-Hydraulic Servo System; Cauchy Mutation; Particle Swarm Optimization; PID Parameters

**Abbreviations:** APSO: Adaptive Particle Swarm Optimization HSS: Hydraulic Servo System; DOE Design of Experiment; BLDCM: Brushless Dc Motor

## Introduction

With the increasing depletion of land-based oil and gas resources, offshore oil has gradually become a strategic priority for coastal countries, and its development has gone through three processes: mechanization, semi-automation, and automation [1-3]. So far, foreign research on drill pipe handling systems has achieved remarkable results and formed a series of drill pipe handling equipment, among which the products of National Oil Company (NOV) are the most representative, and most drilling platforms (vessels) use its supporting equipment [4]. Deepwater drillship is currently the world's advanced offshore oil drilling equipment, which has been developed to the seventh generation. During the work of the drillship, whether the operations of grabbing, transporting, assembling, and discharging of the pipe tools can be completed safely, quickly, stably and efficiently is crucial to whether the drilling speed can be accelerated and thus the drilling cost can be reduced [5]. In deep-water drilling operations, 30% of the time is spent on drill pipe operations, of which the time for catching single rods accounts for 12-20% of the total drilling time, with a lot of room for improvement [6]. The study of the drill pipe discharge system includes the structure and motion control method of the horizontal/vertical drill pipe handling system [7]. The drill pipe discharge system belongs to large lifting equipment, and the working environment is relatively harsh.

Compared with other transmission methods, the hydraulic transmission is more compact and can achieve stable force output, while it is easy to achieve stepless speed regulation. Drill pipe discharge system has the characteristics of large working load, wide range of load variation and high control accuracy requirements, which put

certain requirements on the stability and reliability of the hydraulic system. In this study, the electro-hydraulic servo system of drill pipe discharge system is used to study the corresponding control strategy. PSO algorithm has the advantages of simple operation, robustness, and fast convergence, and it has been used in the literature to optimize nonlinear systems [8-16]. However, the traditional PSO algorithm tends to fall into local optimal solutions. Currently, improved PSO algorithms are introduced with other control methods or intelligent algorithms to deal with complex objects. Zhang et al. applied the classification learning PSO algorithm to the control of a hydraulic hair straightener [17]. Shieh et al. combined particle swarm optimization algorithm with simulated annealing algorithm to deal with nonlinear problems, which improved the efficiency and search quality of the algorithm [18]. Jiang et al. used an improved PSO algorithm to optimize the PID controller parameters of a position control system for a nonlinear hydraulic system [19].

Alfi et al. proposed a novel PSO with adaptive inertia weights to reasonably balance the global exploration by dynamically adjusting the inertia weight of each particle by considering a measure called adjacency index (AI), which simulates a more accurate biological model with inertia weights varying with the number of particles [20]. Considering the mechanical characteristics of BLDCM, Ren et al. proposed an improved PSO algorithm, which is applied to the speed control of brushless DC motor (BLDCM) servo system [21]. To solve the problem that the PID controller parameters are difficult to regulate complex chaotic systems, Huang et al. introduced the uncontrolled chaotic system into the PSO algorithm and proposed an improved dynamic chaotic PSO algorithm [22]. Wang et al. proposed a PSO for PID parameter tuning of two-zone power system PID controller design with multi-objective optimization characteristics [23]. Jiang et al. proposed an adaptive particle swarm optimization (APSO) algorithm to optimize the stability and setup time of the fourth generation grate cooler scraper during the speed regulation process [24]. Aboelela et al. achieved a nonlinear simulation model of the hydraulic servo system (HSS) [25]. Azmi et al., aimed to improve the PSO-PID tuning algorithm by combining the tuning process with a variable weight grayscale-Taguchi design of experiment (DOE) method. It is difficult to achieve the desired control effect on the outlet water temperature using the conventional control algorithm [26]. Long et al. proposed an improved PSO (IPSO) fuzzy PID control strategy to control the outlet water temperature of the air-source heat pump collector control system [27].

Feng et al. proposed an improved PSO algorithm to optimize the coefficients of the proportional-integral derivative (PID) controller to solve the trajectory tracking accuracy problem [28]. For the stability control problem of under-excited mechanical systems, a nonlinear PSO algorithm based on inertia weights of sinusoidal functions was proposed to optimize the parameters of the PID controller (NPSO-PID), solving the problem of under-excited mechanical systems based on the inability to build an accurate mathematical model [29]. Even though researches have obtained high performance of the algorithm and produced quality solutions in practical applications, there is still room for additional enhancement of the PSO performance for solving electro-hydraulic servo system problems. In this study, a mathematical model is established for the electro-hydraulic servo system of drill pipe discharge system, and the transfer function of the electro-hydraulic servo system is obtained by solving according to the parameters of each component. In order to address the shortcomings of the standard PSO algorithm, which is easy to fall into the local optimum, effective measures are introduced to obtain the improved PSO algorithm, and the two PSO algorithms are tested separately by using eight commonly used test functions. The results show that the improved PSO algorithm achieves better control effect on the rectification of PID parameters.

## Electro-hydraulic Servo System Control Model

The diagram of the operation principle of the electro-hydraulic servo system is shown in Figure 1. The hydraulic pump, electro-hydraulic servo valve, hydraulic cylinder and other components form a closed circuit through the pipeline. The displacement sensor is used to collect the displacement signal of the hydraulic cylinder in real time and obtain the deviation signal by comparing it with the given displacement signal, and then control the movement of the electro-hydraulic servo valve spool through the amplification and conversion of the proportional amplifier, which in turn changes the flow rate of the hydraulic circuit and makes the hydraulic cylinder move to the desired position. The structure sketch of the valve-controlled asymmetric hydraulic cylinder is shown in Figure 2. The use of an asymmetric servo valve can effectively avoid sudden jumps in commutation pressure and enhance the load-bearing capacity of the hydraulic cylinder.

 **DOI:** 10.26717/BJSTR.2023.51.008066

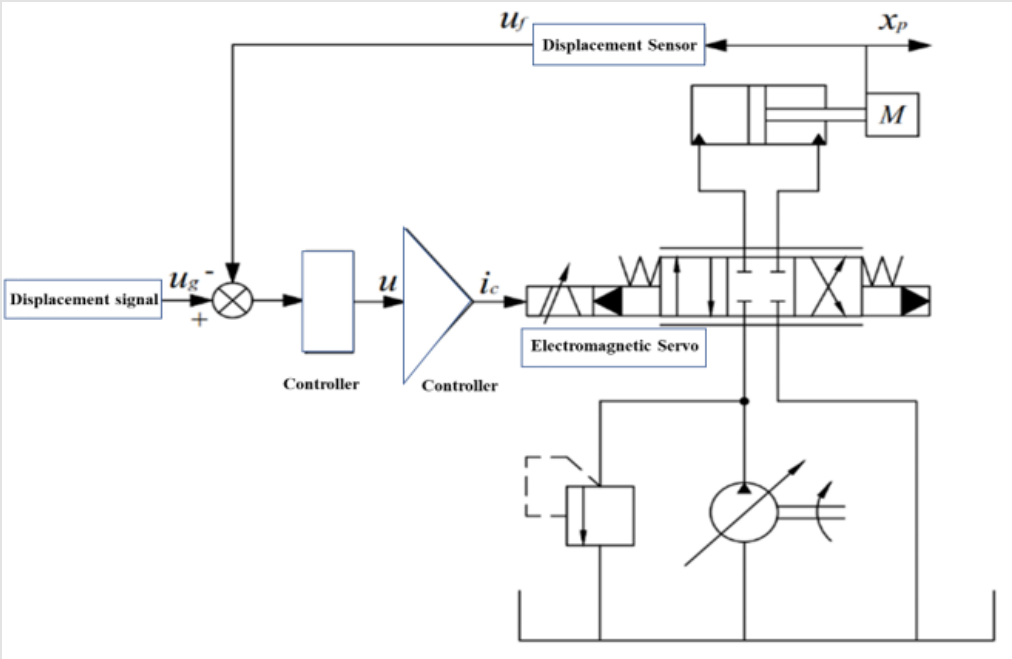


**Figure 1:** Electro-hydraulic servo system working principle diagram.

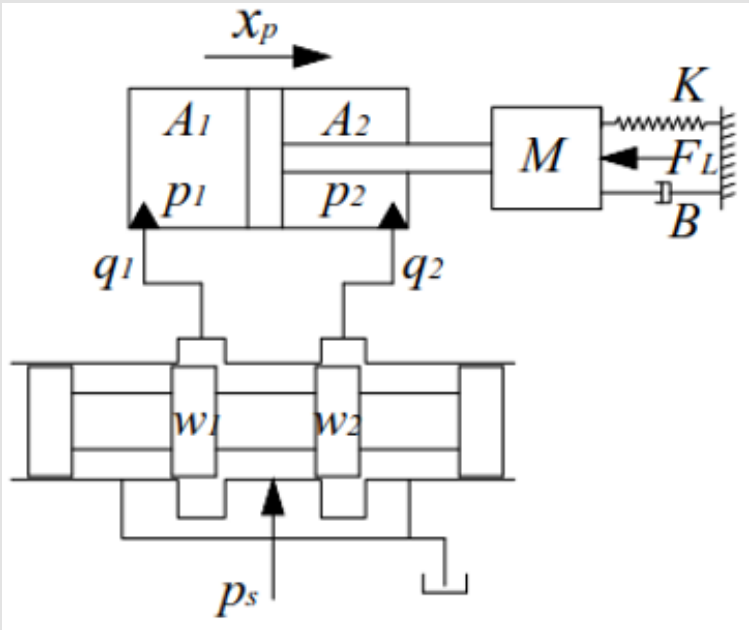


**Figure 2:** Sketch of valve-controlled asymmetric hydraulic cylinder structure.

### Servo Amplifier Mathematical Model

Servo amplifiers play an important role in electro-hydraulic proportional control by amplifying the deviation control signal into a current signal that can drive an electro-hydraulic servo valve. In the modeling analysis of electro-hydraulic servo systems, the servo amplifier is usually regarded as a proportional link. The input signal of the servo amplifier is a voltage signal, and the output signal is a current signal that controls the motion of the servo valve, and its proportional Servo amplifiers play an important role in electro-hydraulic proportional control by amplifying the deviation control signal into a current signal that can drive an electro-hydraulic servo valve. In the modeling analysis of electro-hydraulic servo systems, the servo amplifier is usually regarded as a proportional link. The input signal of the servo amplifier is a voltage signal, and the output signal is a current signal that controls the motion of the servo valve, and its proportional gain is expressed in $K_a$ . The mathematical model is shown as follows.

$$G_a(s)=\frac{I(S)}{U(S)}=K_a \quad (1)$$

### Electro-Hydraulic Servo Valve Mathematical Model

The electro-hydraulic servo valve is responsible for converting electrical signals into hydraulic signals and is the key component to achieve electro-hydraulic conversion. In the analysis of the modeling of the electro-hydraulic servo valve, the dynamic characteristics are usually represented by second-order oscillation links [3], while ignoring its dead zone characteristics. The input signal of the electro-hydraulic servo valve is the current signal output from the pre-servo amplifier, and the output signal is the displacement of the spool, whose mathematical model is shown in Eq. (2).

$$G_v(s)=\frac{X_v(S)}{I(S)}=\frac{K_v}{\frac{s^2}{\omega_v^2}+\frac{2\xi_v}{\omega_v}s+1} \quad (2)$$

in which, $K_v$ servo valve gain (m/A); $\omega_v$ servo valve inherent frequency (rad/s); $\xi_v$ servo valve damping ratio.

### Hydraulic Cylinder Mathematical Model

The mathematical model of the servo valve-controlled hydraulic cylinder system is determined by the load flow equation, the flow continuity equation, and the force balance equation.

**Load pressure and Load Flow Rate:** When modeling the valve-controlled hydraulic cylinder, two important physical quantities are involved, which are load pressure $PL$ and load flow rate $qL$ . For load pressure and load flow rate, there exist various forms of definitions, and for valve-controlled symmetrical hydraulic cylinder, they are usually defined as shown in Eq. (3) and (4).

$$PL=P_1+P_2 \quad (3)$$

$$qL=\frac{q_1+q_2}{2} \quad (4)$$

in which, $P_1$ , $P_2$ -- hydraulic cylinder inlet and outlet pressure (MPa); $q_1$, $q_2$ -- hydraulic cylinder inlet and outlet flow ($m^3$).For valve-controlled asymmetric hydraulic cylinders, the above defined form will result in the servo valve power being less than the hydraulic cylinder power, which violates the law of energy conservation and will lead to an invalid design. According to the literature [5], the load pressure and load flow are defined as shown in Eq. (5) and (6).

$$PL=P_1-mP_2 \quad (5)$$

$$qL=\frac{q_1+mq_2}{1+m^2} \quad (6)$$

in which, m - rodless cavity to rod cavity area ratio.

**Load Flow Equation:** Set the electro-hydraulic servo valve right position energized, that is, the direction of positive when the piston of the hydraulic cylinder moves to the right, according to the pressure-flow equation can be obtained from the rodless chamber and rod chamber flow equation as shown in Eq. (9) and (10).

$$q_1=C_{d1}\omega_1 X_v\sqrt{\frac{2(p_s-p_1)}{\rho}} \quad (7)$$

$$q_2=C_{d2}\omega_2 X_v\sqrt{\frac{2(p_s-p_0)}{\rho}} \quad (8)$$

in which, $C_{d1}$- the flow coefficient from servo valve P port to A port; $C_{d2}$ - the flow coefficient from servo valve B port to T port; $\grave{u}_1$ - the area gradient from servo valve P port to A port (m); ω- the area gradient from servo valve B port to T port (m); $x_v$ - the spool displacement (m); $p_s$ - the system supply pressure (MPa); $p_0$ - the system return pressure (MPa); $\rho$ - the oil density ($m^3$/s). Eq. (7) and (8) shows that, $q_L$ as a function of the spool displacement $x_v$ and the load pressure $p_L$, the linearization can be obtained as shown in Eq. (9).

$$q_L = K_q x_v - K_c p_L \quad (9)$$

in which, $K_q$ --servo valve flow gain; $K_c$ --servo valve pressure-flow coefficient.

**Flow Continuity Equation:** Assuming that the bulk modulus of elasticity of hydraulic oil, oil temperature is a constant, the hydraulic cylinder leakage for laminar motion, and ignore the pressure loss of the pipeline, according to the basic knowledge of fluid transmission, the flow continuity equation of the hydraulic cylinder can be known as shown in Eq. (10).

$$\sum q_i - \sum q_0 = \frac{d_v}{d_t} + \frac{v}{\beta_e}\frac{dp}{dt} \quad (10)$$

in which, $\sum q_i$ - the total flow into the hydraulic cylinder ($m^3$/s); $\sum q_o$ - the total flow out of the hydraulic cylinder ($m^3$/s); V - the volume of the control chamber (m3); $\hat{a}_e$ - the bulk modulus of fluid elasticity ((N/$m^2$)-Pa); p - the pressure in the control chamber (MPa). According to Figure 2 and Eq. (10), the hydraulic cylinder flow continuity equation is obtained as shown in Eq. (11) and (12).

$$q_L = A_1 \frac{dx_P}{dt} + C_{ip}\left(p_1 - p_2\right) + C_{epP_1} + \frac{v_1}{\beta_e}\frac{dp_1}{dt} \quad (11)$$

$$q_L = A_1 \frac{dx_P}{dt} + C_{ip}\left(p_1 - p_2\right) + C_{epP_1} + \frac{v_1}{\beta_e}\frac{dp_1}{dt} \quad (12)$$

in which, A1 - hydraulic cylinder rodless cavity area ($m^2$); A2 - hydraulic cylinder rodless cavity area ($m^2$); $x_p$ - hydraulic cylinder piston rod displacement (m); $c_{ip}$ - hydraulic cylinder internal leakage coefficient ($m^3$/s-Pa-1); $c_{ep}$ - hydraulic cylinder external leakage coefficient ($m^3$/s-Pa-1); V1 - hydraulic cylinder rodless cavity volume (m3); V2 - hydraulic cylinder rodless cavity volume ($m^3$). Assuming that the initial volumes of the rodless and rodged chambers of the hydraulic cylinder are $V_{10}$ and $V_{20}$, respectively, as shown in Eq. (13) and (14).

$$V_1 = V_{\mathbb{0}} + A_1 x_p \quad (13)$$

$$V_2 = V_{20} - A_2 x_p \quad (14)$$

The load flow expressions are obtained by combining Eq. (6), (11), (12), (13) and (14) as follows.

$$q_L = A_1\frac{dx_p}{dt} + \frac{1+m}{1+m^2}C_{ip}\left(p_1 - p_2\right) + \frac{1}{1+m^2}C_{ep}\left(p_1 - mp_2\right) + \frac{1}{1+m^2}\frac{V_{10}}{\beta_e}\frac{dp_1}{dt} - \frac{m}{1+m^2}\frac{V_{20}}{\beta_e}\frac{dp_2}{dt} + \frac{A_1 x_p}{\beta_e}\left(\frac{dp_1}{dt} + m^2\frac{dp_2}{dt}\right) \quad (15)$$

Due to the leakage coefficient in the hydraulic cylinder is very small, can be approximated by taking $C_{ip}\left(p_1 - p_2\right) = C_{ip}\left(p_1 - mp_2\right)$; set the hydraulic cylinder two chambers initial volume is the same, that is $V_{10} = V_{20} = \frac{V_t}{2}$ (Vt) for the hydraulic cylinder equivalent volume), then $A_1 x_p << \frac{V_t}{2}$, $d_{p1}$ and $d_{p2}$ the opposite sign, the fluid volume elastic modulus is very large, the last term of the formula (15) can be ignored. The deformation of Eq. (15) can be obtained as shown in Eq. (16).

$$q_L = A_1\frac{dx_p}{dt} + \frac{1+m}{1+m^2}C_{ip}p_L + \frac{1}{1+m^2}C_{ep}p_L + \frac{1}{1+m^2}\frac{V_t}{2\beta_e}\frac{dp_L}{dt} \quad (16)$$

**Force Balance Equation:**

The hydraulic cylinder is mainly subjected to inertia force, viscous force, nonlinear spring force, external load force and nonlinear friction force. The piston rod is selected as the object of study and the force balance equation is obtained as shown in Eq. (17).

$$p_1 A_1 - p_2 A_2 = p_L A_1 = M\frac{d^2 x_p}{dt^2} + B_c\frac{dx_p}{dt} + K_c x_p + F_L + F_f \quad (17)$$

in which, M - load mass (kg); $B_c$ - damping coefficient of the load (N-s/m); $K_c$ - elasticity coefficient of the load (N/s); $F_L$ - load force (N); $F_f$ - nonlinear friction force (N).

**Transfer Function:** For Eq. (9), (16), (17), both sides simultaneously take the Rasch transform to obtain the set of equations shown in Eq. (18) and (19).

$$\begin{cases} Q_L(s) = K_q x_v(s) + K_c P_L(s) \\ Q_L(s) = A_1 s X_p(s) + \frac{1+m}{1+m^2}C_{ip}P_L(s) + \frac{1}{1+m^2}C_{ep}P_L(s) + \frac{1}{1+m^2}\frac{V_t}{2\beta_e}sP_L(s) \\ A_1 P_L(s) = Ms^2 X_p(s) + B_c s X_p(s) + K_c X_p(s) + F_L(s) + F_f(s) \end{cases} \quad (18)$$

$$X_p(s) = \frac{\frac{K_q}{A_1}x_v - \frac{K_{ce}}{A_1^2}\left(1 + \frac{V_t}{2(1+m^2)\beta_e K_{ce}}s\right)\left(F_L + F_f\right)}{\frac{V_t M}{2(1+m^2)\beta_e A_1^2}s^3 + \left[\frac{MK_{ce}}{A_1^2} + \frac{B_c V_t}{2(1+m^2)\beta_e A_1^2}\right] + \left[\frac{K_c V_t}{2(1+m^2)\beta_e A_1^2} + \frac{B_c K_{ce}}{A_1^2} + 1\right]s + \frac{K_c K_{ce}}{A_1^2}} \quad (19)$$

in which, $K_{ce} = K_c + \frac{1+m}{1+m^2}C_{ip} + \frac{C_{ep}}{1+m^2}$, is the hydraulic system flow pressure coefficient.

Defined separately. $\omega_h = \sqrt{\frac{2(1+m^2)\beta_e A_1^2}{MV_t}}$ is the undamped intrinsic frequency of the hydraulic system; $\xi_h = \frac{K_{ce}}{A_1}\sqrt{\frac{(1+m^2)\beta_e M}{2V_t}} + \frac{B_c}{2A_1}\sqrt{\frac{V_t}{2(1+m^2)\beta_e M}}$ is the damping ratio of the hydraulic system; $\omega_1 = \frac{2(1+m^2)\beta_e K_{ce}}{V_t}$ is the turning frequency. Then, Eq. (19) can be reduced to a general expression shown in Eq. (20).

$$X_p(s) = \frac{\frac{K_q}{A_1}x_v - \frac{K_{ce}}{A_1^2}\left(1+\frac{1}{\omega_1}s\right)\left(F_L+F_f\right)}{s\left(\frac{s^2}{\omega_h^2}+\frac{2\zeta_h}{\omega_h}s+1\right)} \quad (20)$$

### Displacement Sensor Mathematical Model

The displacement sensor input signal is the hydraulic cylinder displacement, and the output signal is the voltage signal. Since the displacement sensor bandwidth is much higher than the system bandwidth, it can be regarded as a proportional link, and its mathematical model is expressed shown in Eq. (21).

$$G_f(s) = \frac{U_f(s)}{X_p(s)} = K_f \quad (21)$$

### Mathematical Model of Electro-Hydraulic Servo System

The mathematical model of each module obtained from the above analysis is connected according to the direction of signal flow, and the block diagram of electro-hydraulic servo system transfer function is shown in Figure 3. Without considering load and friction, the open-loop transfer function is obtained as shown in Eq (22).

$$G(s) = \frac{X_p(s)}{U(s)} = \frac{K_a K_v K_q K_f / A_1}{s\left(\frac{s^2}{\omega_v^2}+\frac{2\zeta_v}{\omega_v}s+1\right)\left(\frac{s^2}{\omega_h^2}+\frac{2\zeta_h}{\omega_h}s+1\right)} \quad (22)$$

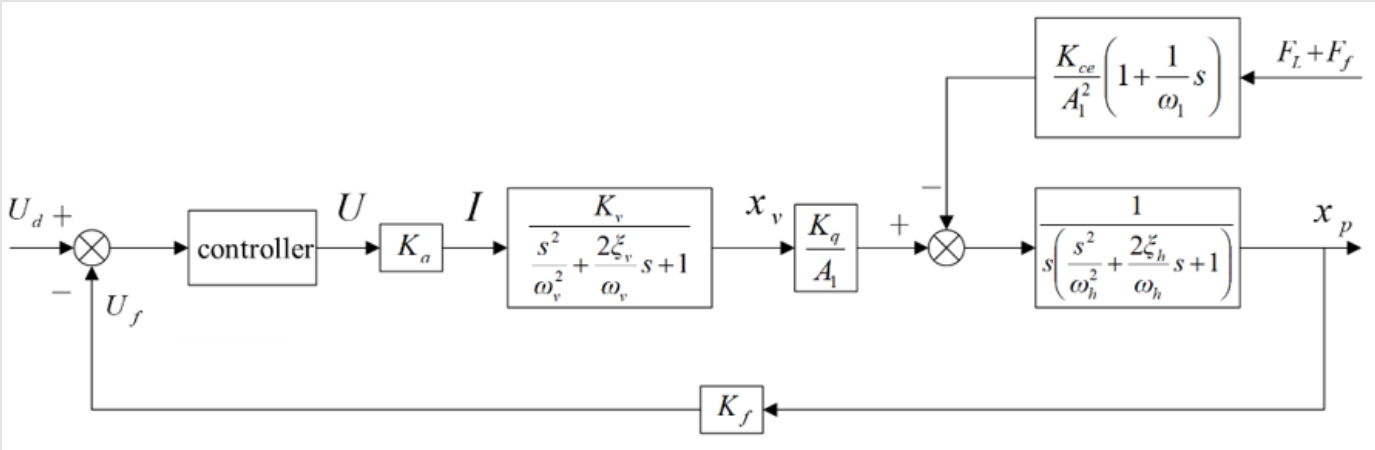


**Figure 3:** Block diagram of electro-hydraulic servo system transfer function.

## Improved PSO Algorithm based on Cauchy Variation

### Standard Particle Swarm Optimization Algorithm

The PSO algorithm considers each individual of the biota as a particle, and the biota is not sure of the specific location of the food in the foraging process, but can perceive the location relationship with the food, and the particles keep approaching the food through their own memory and mutual communication until they find the food, and the biota foraging process is a gradually converging process. The PSO algorithm can be described in mathematical language as follows: in the D-dimensional space, there are m particles randomly distributed, and the population they form can be denoted as X($x_1$, $x_2$,..., $x_m$,), the position of the i-th particle at time of k can be expressed as a D-dimensional vector, which is $X_i^k = \left(X_{i1}^k, X_{i2}^k, ..., X_{iD}^k\right)$. The corresponding velocity is expressed as $V_i^k = \left(v_{i1}^k, v_{i2}^k, \cdots, v_{iD}^k\right)$ . The position of each particle can be regarded as a candidate solution to the objective problem, and the merit of the candidate solution is evaluated by the fitness

function. The best position that a single particle swarm can find at moment k is $P_i^k = \left(p_{i1}^k, p_{i2}^k, \cdots, p_{iD}^k\right)$ , and the best position of the whole population at moment k is $P_g^k = \left(p_{g1}^k, p_{g2}^k, \cdots, p_{gD}^k\right)$ , and according to the above rules, the velocity and position of PSO are updated as shown in Eq. (23) and (24).

$$v_{id}^{k+1} = v_{id}^k + c_1 \cdot r_1 \left(p_{id}^k - x_{id}^k\right) + c_2 \cdot r_2 \left(p_{gd}^k - x_{gd}^k\right) \quad (23)$$

$$x_{id}^{k+1} = x_{id}^k + v_{id}^{k+1} \quad (24)$$

In this formula, c1 is the individual learning factor, which is the coefficient of the particle tracking individual historical optimum, and c2 is the social learning factor, which indicates the empirical learning of the particle to the particle population. c1 and c2 are usually taken as positive real numbers between [0,2]; r1 and r2 are random numbers in the range of [0,1]; in order to prevent the particle's speed from going too fast or its position from crossing the boundary, the speed and position of the particle are constrained by setting $x_{id}^k \in [V_{\min}, V_{\max}]$, $v_{id}^k \in [v_{\min}, v_{\max}]$.In 1998, Shi and Eberhart introduced the inertia weight ω into the PSO algorithm [8], which is used to improve the convergence of the PSO algorithm and make its performance better, and the improved PSO algorithm is called the standard PSO algorithm, whose position update formula remains unchanged, and the velocity update formula is modified shown in Eq. (25).

$$v_{id}^{k+1} = \omega v_{id}^k + c_1 \cdot r_1 \left(p_{id}^k - x_{id}^k\right) + c_2 \cdot r_2 \left(p_{gd}^k - x_{gd}^k\right) \quad (25)$$

From the Eq. (25), it can be seen that the update of velocity in the PSO algorithm is determined by three aspects. Among them: It is influenced by the inertia weight, which is a balance between the global search ability and the local search ability; $c_1 \cdot r_1 \left(p_{id}^k - x_{id}^k\right)$ is the exchange of information about the particle itself, which determines the next direction of motion by comparing the current position with the best position of the individual; $c_2 \cdot r_2 \left(p_{gd}^k - x_{gd}^k\right)$ is the exchange of information between the particle and the global information, which helps the particle to jump out of the local optimum and make it find the global optimum quickly and accurately.

## Improved Particle Swarm Optimization Algorithm

Due to the standard particle swarm algorithm has no mechanism for mutation, its merit-seeking process is achieved through cooperation and competition among the particles of the population, so when a single particle is constrained by local extremes that are not found by other particles, it is easy to fall into a local optimum and cannot obtain a global optimum [30,31]. Therefore, the introduction of the Cauchy variation updates the position of the standard PSO algorithm to improve its optimality finding ability, and the Cauchy variation produces a larger variation step, giving it a higher probability of escaping the local optimum. The probability density function of the one-dimensional Cauchy distribution is given in Eq. (26).

$$X_i = \left(x_{i1}, x_{i2}, \cdots, x_{in}\right) \quad (26)$$

in which, t is a scaling parameter, and it is greater than 0.

According to the traditional idea of variational operators, for individual $X_i = \left(x_{i1}, x_{i2}, \cdots, x_{in}\right)$ , the variational formula is shown in Eq. (27).

$$x_{ij} = x_{ij} + \eta * C\left(0,1\right) \quad (27)$$

in which, j=1, 2, ..., n; η is a constant controlling the variation step; and C (0,1) denotes the random number generated by the Cauchy distribution function when the scaling parameter t is 1. Introducing the Cauchy variation operator and taking the variation step η as the square root of the absolute value of the position, the position update formula of the IPSO is obtained shown in Eq. (28) and (29).

$$x_{id}^{k+1} = x_{id}^k + v_{id}^{k+1} \quad (28)$$

$$x_{id}^{k+1} = x_{id}^k + v_{id}^{k+1} \quad (29)$$

The steps of the IPSO algorithm are described as shown in Figure 4.

| The steps of the improved particle swarm optimization algorithm | |
|---|---|
| Step1: | Set the particle swarm size, problem solving dimension Dim, maximum iteration MaxIter, inertia weight $\omega$, individual experience learning factor c1, social experience learning factor c2, velocity and position boundaries, and initialize the particles and their velocities. |
| Step2: | Evaluating the first generation of particle fitness to obtain the individual optimum $P1$ and the global optimum $Pg$. |
| Step3: | When the number of iterations exceeds the maximum number of iterations (Iter>MaxIter), stop the search, and output the extreme point at the same time, otherwise go to Step4 |
| Step4: | IPSO does a global search: |
| | for $i$=1:SwarmSize |
| | Update the velocity of particle $x_i$ according to Eq. (23). |
| | Update the position of particle $x_i$ according to Eq. (28), (29). |
| | Calculation of the adaptation value of particle $x_i$. |
| | Update the individual optimal value $Pi$ of particle $x_i$. |
| | Updating the optimal value $Pg$ of the particle population. |
| | End for |
| Step5: | Iter=Iter+1， return to Step3 |

**Figure 4:** The steps of the improved PSO algorithm.

## Experimental Verification

### Particle Swarm Optimization Algorithm Model Validation

In order to verify the effectiveness of the improved PSO algorithm and evaluate its performance in terms of merit-seeking ability and convergence speed, eight test functions as shown in Table 1 are introduced for testing, among which F1~F4 are single-peak test functions and F5~F8 are multi-peak test functions. The simulation results of the standard PSO and the IPSO for solving the test functions F1 to F8 are shown in Table 2. The "optimal value" is the best optimized value obtained from 50 times of solving, "average value" is the average of the optimized values obtained from 50 times of solving, and "standard deviation" is the mean squared deviation based on the average value. The "standard deviation" is the mean squared deviation based on the mean value. As can be seen from Table 2, IPSO solves the eight test functions, except for F2, and the obtained optimal values, mean and standard deviation are significantly better than PSO; for function F2, the optimal values obtained by IPSO and PSO are 1, which is the theoretical optimal value of the function, but the mean and standard deviation of IPSO are better than PSO; through comparison, it can be found that the solution performance of the IPSO is substantially improved. In order to compare the convergence speed of PSO and IPSO, the eight test functions were solved 50 times respectively, and the average value of the adaptation value after each iteration was obtained, and the adaptation curves of the PSO and IPSO optimization test function process were plotted, as shown in Figures 5-12.

**Table 1:** List of test functions.

| Name of function | Function expressions | Superiority-seeking interval | extremum |
|---|---|---|---|
| Dixon-Price | $F_1=(x_1-1)^2+\sum_{i-2}^{d} i\left(2x_i^2-x_{i-1}\right)^2$ | $x\in[-10,10]^d$ | $F_{\min}=0$ |
| Exponential | $F_2=-\exp\left(-0.5\sum_{i-1}^{d}x_i^2\right)$ | $x\in[-1,1]^d$ | $F_{\min}=-1$ |
| Rosenbrock | $F_3=\sum_{i=1}^{d-1}\left[100\left(x_{i+1}-x_i^2\right)^2+\left(x_i-1\right)^2\right]$ | $x\in[-30,30]^d$ | $F_{\min}=0$ |
| Sphere | $F_4=\sum_{i-1}^{d}x_i^2$ | $x\in[-100,100]^d$ | $F_{\min}=0$ |
| Griewank | $F_5=\sum_{i=1}^{d}\frac{X_i^2}{4000}-\prod_{i=1}^{d}\cos\left(\frac{x_i}{\sqrt{i}}\right)+1$ | $x\in[-600,600]^d$ | $F_{\min}=0$ |

| | | | |
|---|---|---|---|
| Rastrigin | $F_6 = \sum_{i=1}^{d}\left(x_i^2 - \cos(2\pi x_i) + 10\right)$ | $x \in [-5.12, 5.12]^d$ | $F_{\min} = 0$ |
| Salomon | $F_7 = 1 - \cos\left(2\pi\sqrt{\sum_{i=1}^{d} x_i^2}\right) + 0.1\sqrt{\sum_{i=1}^{d} x_i^2}$ | $x \in [-100, 100]^d$ | $F_{\min} = 0$ |
| Ackley | $F_8 = -20\exp\left(-0.2\sqrt{\frac{1}{d}\sum_{i-1}^{d} x_i^2}\right) - \exp\left(\frac{1}{d}\sum_{i-1}^{d}\cos(2\pi x_i)\right) + 20$ | $x \in [-100, 100]^d$ | $F_{\min} = 0$ |

**Table 2:** Simulation test result.

| Function No. | Optimum value | | Average value | | Standard deviation | |
|---|---|---|---|---|---|---|
| | PSO | IPSO | PSO | IPSO | PSO | IPSO |
| F1 | 1.62E-01 | 9.73E-02 | 7.32E-01 | 2.34E-01 | 2.57E-01 | 2.97E-02 |
| F2 | 1.00E+00 | 1.00E+00 | 0.999966 | 1.00E+00 | 8.14E-06 | 0.00E+00 |
| F3 | 5.60E-01 | 7.82E-08 | 1.50E+02 | 1.20E-02 | 5.96E+02 | 2.38E-02 |
| F4 | 1.70E-04 | 3.72E-09 | 5.23E-02 | 4.32E-04 | 1.22E-01 | 1.10E-03 |
| F5 | 3.97E-02 | 2.54E-08 | 3.18E-01 | 4.52E-02 | 2.09E-01 | 1.39E-01 |
| F6 | 3.99E+00 | 3.45E-07 | 1.83E+01 | 8.46E-04 | 7.79E+00 | 1.30E-03 |
| F7 | 3.00E-01 | 1.07E-04 | 7.48E-01 | 2.57E-02 | 3.09E-01 | 3.72E-02 |
| F8 | 6.79E-02 | 1.73E-04 | 2.69E+00 | 6.61E-03 | 9.64E-01 | 7.08E-03 |

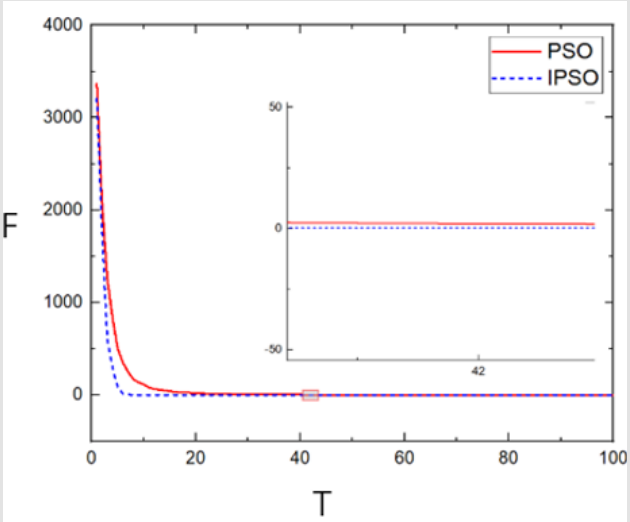


**Figure 5:** Fitness curve of PSO and IPSO optimizing function F1.

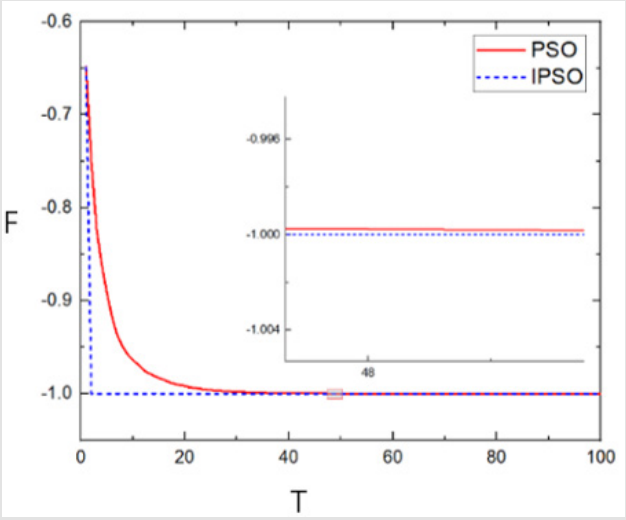


**Figure 6:** Fitness curve of PSO and IPSO optimizing function F2.

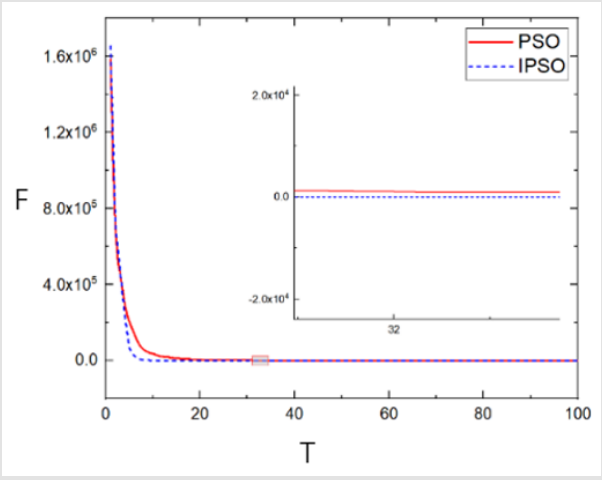


**Figure 7:** Fitness curve of PSO and IPSO optimizing function F3.

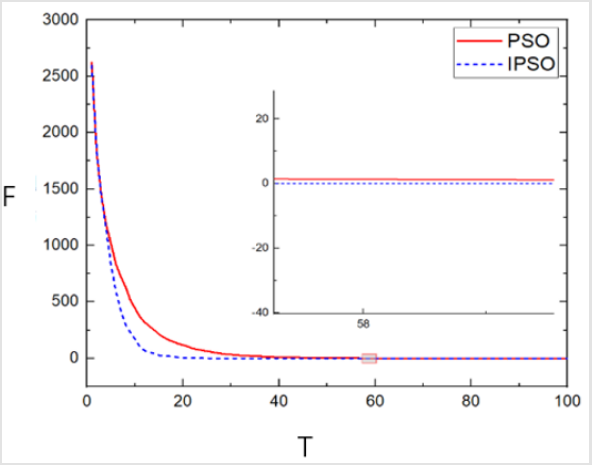


**Figure 8:** Fitness curve of PSO and IPSO optimizing function F4.

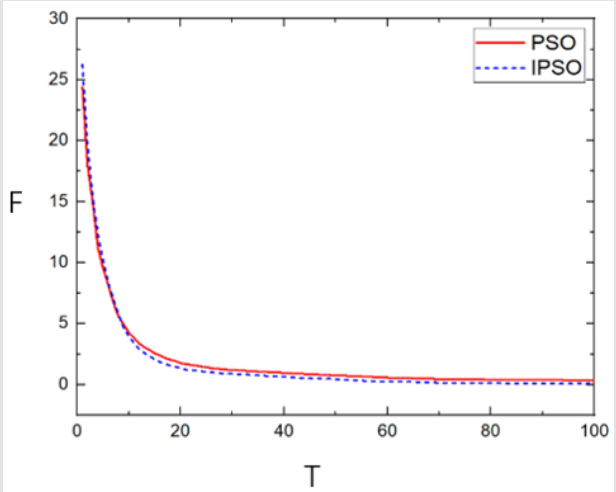


**Figure 9:** Fitness curve of PSO and IPSO optimizing function F5.

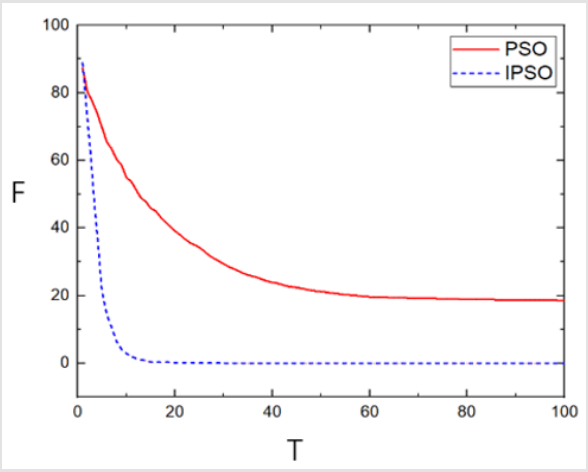


**Figure 10:** Fitness curve of PSO and IPSO optimizing function F6.

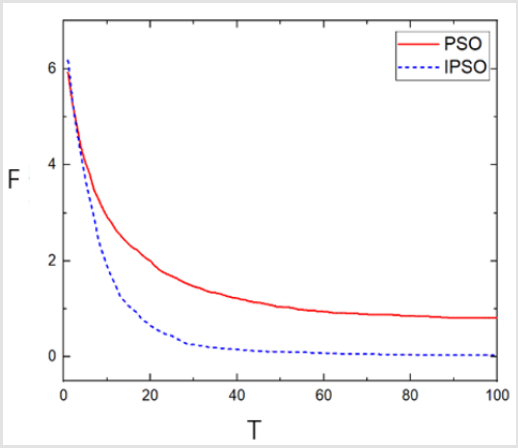


**Figure 11:** Fitness curve of PSO and IPSO optimizing function F7.

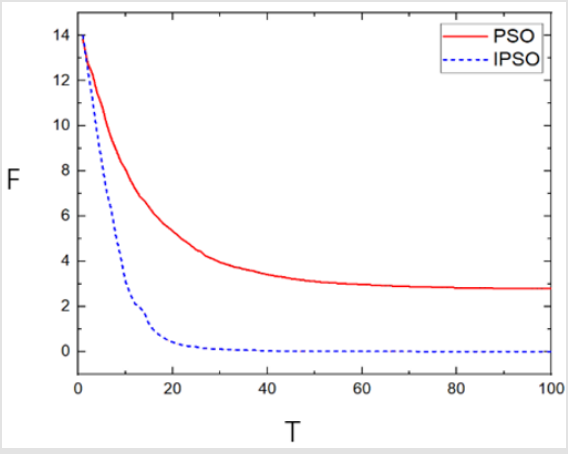


**Figure 12:** Fitness curve of PSO and IPSO optimizing function F8.

As can be seen from these Figures, for the single-peak test functions F1, F3, and F4, the difference in performance between PSO and IPSO is not significant at the beginning, which is because the adaptation values of the particles are poor at this time, and the improved PSO does not improve them very well. For the multi-peak test functions F5~F8, the convergence speed is significantly improved in all cases. In addition, by comparing the adaptation value curves of PSO and IPSO in optimizing the test functions, it can be found that the final adaptation values obtained by IPSO are better than those of PSO. Through the above simulation experiments, it can be seen that the improved PSO has significantly improved its optimization finding accuracy and convergence speed when solving single-peak and multi-peak problems.

## Adjustment of PID Parameters Based on Particle Swarm Optimization Algorithm

**PID Parameter Adjustment Principle:** PID parameter tuning is a more common industrial control problem, which aims to find the optimal values of Kp, Ki, and Kd parameters to obtain the best control performance, which can be essentially summarized as a global optimization search problem.

$$e(t) = r(t) - y(t)$$

$$u(t) = K_p e(t) + K_i \int_0^t e(t)dt + K_d \frac{de(t)}{dt}$$

in which, e(t) is the system error, r(t) is the desired output value, y(t) is the actual output value, and Kp, Ki, and Kd are the proportional, integral, and differential coefficients respectively. PID control eliminates the error by simultaneously performing proportional, integral, and differential calculations on the system error e(t) to make the system act as closely as possible to the given signal. In modern control, in order to avoid the defects of traditional control methods, intelligent algorithms are introduced to adjust the PID parameters through continuous learning and iteration processes to achieve the desired control effect. The most commonly used control algorithms include fuzzy algorithms, neural network algorithms, genetic algorithms, particle swarm algorithms, etc. Optimization of PID parameters using particle swarm algorithm can be regarded as an optimization-seeking problem of dimension 3. The components of each particle's position information in three dimensions represent the three parameter values Kp, Ki, and Kd of the PID, and a set of most suitable PID parameter values are selected by continuous iteration using particle swarm in a given search space to optimize the performance index of the system.

**Electro-Hydraulic Servo System Transfer Function Solution:** Eq. (22) gives the mathematical model of the electro-hydraulic servo system open-loop transfer function, which needs to be calculated according to the actual parameters of each component to determine the transfer function, to lift the hydraulic cylinder as an example, the parameters are shown in Table 3. In Table 3, the block diagram of the electro-hydraulic servo system is obtained as shown in Figure 13. The open-loop transfer function of the system is obtained as:

$$G(s) = \frac{0.0962}{s\left(\frac{s^2}{600^2} + \frac{1}{600}s + 1\right)\left(\frac{s^2}{261^2} + \frac{0.023}{261}s + 1\right)} = \frac{0.0962}{4.078\times10^{-11}s^5 + 2.471\times10^{-8}s^4 + 1.76\times10^{-5}s^3 + 0.001755s^2 + s}$$

**Table 3:** Electro-hydraulic servo system parameters.

| Symbol | Parameter | Numerical value |
|---|---|---|
| $K_a$ | Magnification factor | 0.2A·V$^{-1}$ |
| $K_v$ | Servo valve gain | 3.06×10$^{-3}$ m·A$^{-1}$ |
| $K_q$ | Flow gain | 1m$^2$·s$^{-1}$ |
| $\zeta_v$ | Servo valve damping ratio | 0.5 |
| $\omega_v$ | Servo valve inherent frequency | 600rad·s$^{-1}$ |
| $K_f$ | Servo-amplifier gain | 100 |
| $\rho$ | Hydraulic oil density | 850kg·m$^{-3}$ |
| $K_c$ | Servo valve pressure flow coefficient | 3.41×10$^{-12}$ m$^3$·s$^{-1}$·Pa$^{-1}$ |
| $m$ | Rodless chamber to barred chamber area ratio | 0.7 |

| | | |
|---|---|---|
| $C_{ip}$ | Hydraulic cylinder internal leakage coefficient | $4.52\times10^{-14}$ m$^3$ ·s$^{-1}$ ·Pa$^{-1}$ |
| $C_{ep}$ | Hydraulic cylinder external leakage coefficient | $1.05\times10^{-13}$ m$^3$ ·s$^{-1}$ ·Pa$^{-1}$ |
| $\beta_e$ | Effective elastic modulus | $1.7\times10^9$ N ·m$^{-2}$ |
| $A_1$ | Rodless cavity effective area | $6.36\times10^{-3}$m$^2$ |
| $A_2$ | Effective area of rod cavity | $3.24\times10^{-3}$m$^2$ |
| $M$ | Load mass | 1000kg |
| $V_t$ | Equivalent volume of hydraulic cylinder | $3.01\times10^{-3}$m$^3$ |
| $K_f$ | Displacement sensor coefficient | 1 |

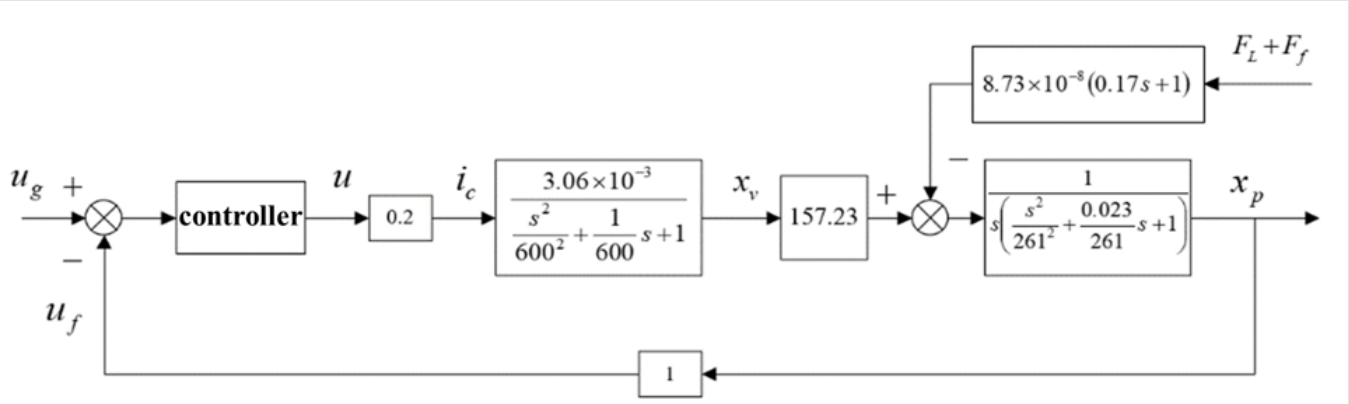


**Figure 13:** Diagram of electro-hydraulic servo system.

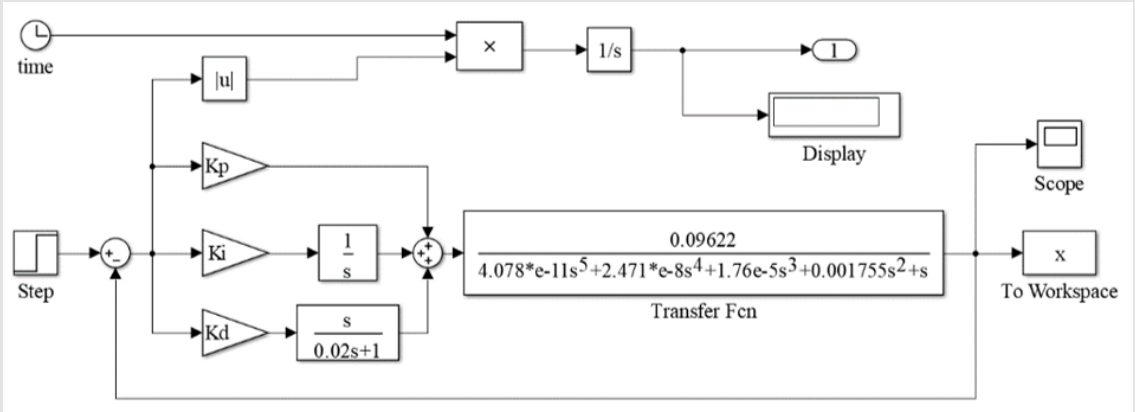


**Figure 14:** PID simulation model.

**Simulink Model Building:** The simulation experiments were performed by writing algorithms in Matlab, building a PID simulation model using Simulink, and running the program to continuously call the PID model to achieve the optimization of PID parameters. The PID simulation model built under Simulink is shown in Figure 14. The upper part is the objective function, the fitness function of the PSO, and the time integration function of the absolute value of the error is chosen as the fitness function in the simulation, with the expression as; the lower part is the PID control model, in which the differential link is replaced by a first-order inertial link approximation to form an incomplete integral PID controller.

**Analysis of Simulation Results:** Simulation experiments were conducted using the standard PSO and the IPSO, respectively, to compare their response curves under step input. When using PSO/IPSO to optimize the PID parameters, the parameters need to be initialized and set as shown in Table 4. Running the program, the optimized PID parameters and performance indexes of the two PSO algorithms are obtained, as shown in Table 5, and the index change curve during 100 iterations is also obtained, as shown in Figure 15. From the Figure 15, it can be seen that when PSO is used to optimize the PID parameters, there is a tendency to fall into local optimum, which greatly affects its convergence speed; IPSO with the introduction of the variant converges faster when it is close to the optimal value, and also the final optimization results are better than PSO. The step response curves of the system after the optimization of the two algorithms are given in Figure 16. From Figure 16 and Table 5, it can be seen that the improved PSO optimizes the PID parameters with a significant improvement in the regulation time, which indicates that the system is more responsive.

**Table 4:** PSO/IPSO optimized PID initial parameter settings.

| Symbol | Parameter | Numerical value |
|---|---|---|
| c1 | Individual Learning Factor | 2 |
| c2 | Social Learning Factor | 2 |
| Dim | Dimension | 3 |
| ω | Inertia factor | 0.6 |
| SwarmSize | Population size | 100 |
| MaxIter | Maximum iterations | 100 |
| $[V_{min},V_{max}]$ | Particle velocity range | [-1,1] |
| $[L_1,U_1]$ | $K_p$ Search range | [0,300] |
| $[L_2,U_2]$ | $K_i$ Search range | [0,300] |
| $[L_3,U_3]$ | $K_d$ Search range | [0,300] |

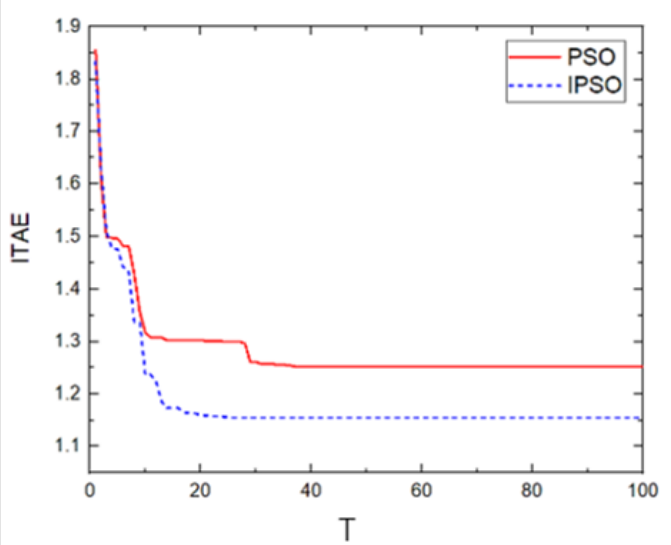


**Figure 15:** ITAE variation curve.

**Table 5:** Optimized PID parameters and performance indicators.

| Method | Kp | Ki | Kd | Rise time | Adjustment time | Number of iterations | ITAE |
|---|---|---|---|---|---|---|---|
| PSO | 24.22 | 0.05 | 0.56 | 1.80s | 3.89s | 42 | 1.2519 |

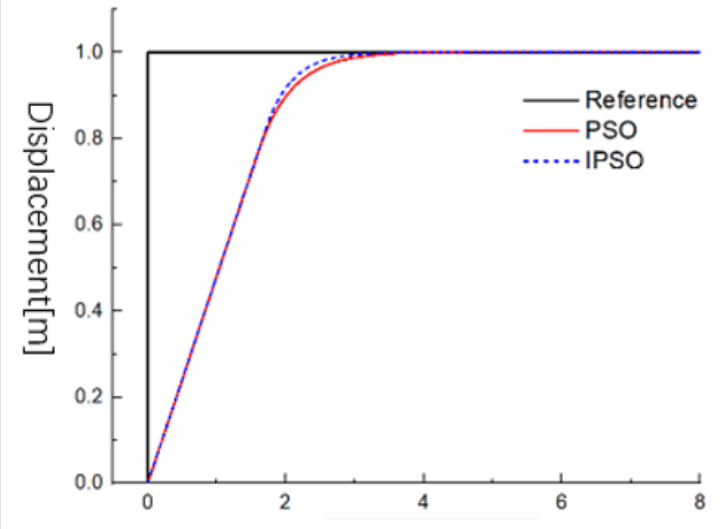


**Figure 16:** System unit step response curve.

## Conclusion

In this paper, according to the schematic diagram of the electro-hydraulic servo system, the transfer functions of the electro-hydraulic servo valve, hydraulic cylinder and other components are established respectively. The mathematical models of each module are connected according to the signal flow direction, and the transfer function of the electro-hydraulic servo system is obtained. By introducing Cauchy mutation, an improved PSO algorithm is proposed, which overcomes the problem that traditional PSO is easy to fall into local optimum. The Simulink simulation model was developed, and it was found through simulation that the IPSO algorithm achieved better control effect on the PID tuning. The simulation results verified the superiority of the IPSO algorithm. In summary, the IPSO is able to obtain high-quality solutions for the corresponding instances with high efficiency. However, the IPSO still has some shortcomings that need to be further investigated. In the next step, the focus will be on further improving the efficiency of the algorithm. In addition, the IPSO can be used for other practical applications.

## Declaration of Competing Interest

The authors declare no conflict of interest.

## Data Availability

The datasets used during the current study are available from the corresponding author on reasonable request.

## Acknowledgment

This research is funded by the Project of Ministry of Industry and Information Technology of the People's Republic of China (Research on the key technology of treatment process for high -flow offshore natural gas, CJ09N20).

## References

1. Chanysheva A, Ilinova A (2021) The future of Russian arctic oil and gas projects: Problems of assessing the prospects. Journal of Marine Science and Engineering 9(5): 528.
2. Pang X Q, Chen Z H, Jia C Z (2021) Evaluation and re-understanding of the global natural gas hydrate resources. Petroleum Science 18(2): 323-338.
3. Liu X, Zhang J, Guo X (2023) A grading evaluation method of shale oil and gas resources. Resources Data Journal 2: 21-34.
4. Rohde K, Berg T, Yost T (2010) Fully Automatic Pipehandling Systems on a 6th-Generation Drilling Vessel.
5. Carpenter C (2022) Matrix Injectivity Achieved in Deepwater Gas-Injector Wells. Journal of Petroleum Technology 74(05): 62-64.
6. Liu Z, He J, Meng Y (2022) Numerical and experimental study on the influence of a moonpool on motion performance and stability of a drillship. Ocean Engineering 262: 112241.
7. Price M E, Randall M T, Sulak K J (2022) Temporal and Spatial Relationships of Yellowfin Tuna to Deepwater Petroleum Platforms in the Northern Gulf of Mexico. Marine and Coastal Fisheries 14(4): e10213.
8. Gad A G (2022) Particle swarm optimization algorithm and its applications: a systematic review. Archives of computational methods in engineering 29(5): 2531-2561.
9. Xing Z, Zhu J, Zhang Z (2022) Energy consumption optimization of tramway operation based on improved PSO algorithm. Energy 258: 124848.
10. Singh N, Singh S B, Houssein E H (2022) Hybridizing salp swarm algorithm with particle swarm optimization algorithm for recent optimization functions. Evolutionary Intelligence, p. 1-34.
11. Song B, Wang Z, Zou L (2021) An improved PSO algorithm for smooth path planning of mobile robots using continuous high-degree Bezier curve. Applied Soft Computing 100: 106960.
12. Sennan S, Ramasubbareddy S, Balasubramaniyam S (2021) T2FL-PSO: Type-2 fuzzy logic-based particle swarm optimization algorithm used to maximize the lifetime of Internet of Things. IEEE Access 9: 63966-63979.

13. Wang F, Zhang H, Zhou A (2021) A particle swarm optimization algorithm for mixed-variable optimization problems. Swarm and Evolutionary Computation 60: 100808.

14. Minh H L, Khatir S, Rao R V (2023) A variable velocity strategy particle swarm optimization algorithm (VVS-PSO) for damage assessment in structures. Engineering with Computers 39(2): 1055-1084.

15. Gao K, Xu W, Zhang H (2020) Relative position and posture detection of hydraulic support based on particle swarm optimization. IEEE Access 8: 200789-200811.

16. Yiyang L, Xi J, Hongfei B (2021) A general robot inverse kinematics solution method based on improved PSO algorithm. IEEE Access 9: 32341-32350.

17. Zhang K, Song J, Li S (2017) Hydraulic straightener control optimizer based on particle swarm with classification learning. J Mech Eng 53: 202-208.

18. Shieh HL, Kuo CC, Chiang CM (2011) Modified particle swarm optimization algorithm with simulated annealing behavior and its numerical verification. Appl Math Comput 218: 4365-4383.

19. Jiang G-Y, Wang Y-Q, Yan X-C (2008) Mathematics Modeling and simulation analysis of dynamic characteristics for hydraulic cylinder controlled by servo-valve. J Sichuan Univ (Eng Sci Ed) 40: 195-198.

20. Alfi A, Modares H (2011) System identification and control using adaptive particle swarm optimization. Appl Math Model 35: 1210-1221.

21. Ren Y, Xu X (2008) Optimization research of PSO-PID algorithm for the design of brushless permanent magnet machines. Fifth IEEE International Symposium on Embedded Computing. IEEE, p. 26-30.

22. Huang Q, Li T, Li Z (2012) Research on PID control technique for chaotic ship steering based on dynamic chaos particle swarm optimization algorithm. Proceedings of the 10th World Congress on Intelligent Control and Automation. IEEE 1639-1643.

23. Wang J (2015) Two regional power system PSO PID Control Research. TELKOMNIKA Indonesian Journal of Electrical Engineering 13(1): 33-41.

24. Jiang C H, Xu H, Wang S H (2016) PID parameter optimization of the grate cooling electro-hydraulic position servo system based on APSO.13th International Computer Conference on Wavelet Active Media Technology and Information Processing (ICCWAMTIP). IEEE, pp. 385-390.

25. Aboelela M A S, Essa M E S M, Hassan M A M (2018) Modeling and identification of hydraulic servo systems. International Journal of Modelling and Simulation 38(3): 139-149.

26. Azmi N I M, Piah K A M, Yusoff W A W (2018) Optimization of PID Parameters Utilizing Variable Weight Grey-Taguchi Method and Particle Swarm Optimization.Conference Series: Materials Science and Engineering. IOP Publishing 319(1): 012012.

27. Long G, Yi Y, Xiaolin R (2020) Research on Temperature Control System Based on IPSO Optimized Fuzzy PID 39th Chinese Control Conference (CCC). IEEE, pp. 2014-2019.

28. Feng H, Ma W, Yin C (2021) Trajectory control of electro-hydraulic position servo system using improved PSO-PID controller. Automation in Construction 127: 103722.

29. Dai P, Zhong P, Liu H (2021) Stabilization control of under-actuated mechanical system based on improved NPSO-PID controller. International Conference on Intelligent Equipment and Special Robots (ICIESR 2021). SPIE 12127: 353-361.

30. Qinghua M A O, Qiang Z (2021) Improved sparrow algorithm combining Cauchy mutation and Opposition-based learning. Journal of Frontiers of Computer Science & Technology 15(6): 1155.

31. Ding M, Huang T Z, Wang S (2019) Total variation with overlapping group sparsity for deblurring images under Cauchy noise. Applied Mathematics and Computation 341: 128-147.

**ISSN: 2574-1241**

DOI: 10.26717/BJSTR.2023.51.008066

**Chao Liu.** Biomed J Sci & Tech Res